Journal of the European Ceramic Society 22 (2002) 1891–1896

www.elsevier.com/locate/jeurceramsoc

Liquid assisted sintering of SiC powders by MW (2.45 GHz) heating

A. Goldstein[a,*], W.D. Kaplan[b], A. Singurindi[a]

[a]*Israel Ceramic and Silicate Institute, Technion City, 32000 Haifa, Israel*
[b]*Department of Materials Engineering, Technion, Israel Institute of Technology, Haifa 32000, Israel*

Received 29 August 2001; accepted 11 November 2001

Abstract

The feasibility of densifying α-silicon carbide powder compacts—based on a liquid assisted sintering approach—by the use of microwave powered furnaces, is examined. Despite the low penetration depth of GHz radiation, it is possible to obtain microwave sintering of SiC. Spatial uniformity of fired state density and warpage/cracking tendency are more dependent on size than in the case of conventional heating. Electromagnetic field intensity spatial variation—related to both the low penetration depth of the carbide and the inherent non-uniformity of the MW's distribution within the applicator—is one of the main factors which negatively affect densification uniformity. Nonetheless, fired state bulk density of 98% t.d. may be achieved in the case of small components. The phase composition of MWed and respectively conventionally sintered specimens is similar and so is the grain size distribution. A larger fraction of the oxide second phase is accumulated in triple points than in the case of resistive furnace firing. While MW sintering of SiC is feasible, it does not seem to generate practical advantages over conventional heating.

Keywords: Carbides; Dielectric properties; Firing; Microwave processing; SiC; Sintering

1. Introduction

The use of microwave and other, lower frequency, radiation powered furnaces, has been under investigation for use in sintering of ceramics.[1–11] The main specific feature of microwave heating (MWH) is that the specimens are subjected to the action of high frequency electromagnetic fields during sintering. This fact has a number of consequences, such as the development of a heat source within the specimen (as opposed to conventional external heating), preferential heating of porous regions, and in some cases plasma formation.[4,5,11–14] Non-thermal effects, such as material flow enhancement along interfaces, which influence solid state sintering, are deemed possible.[3–6,15–17] Dissolution/precipitation processes, which control liquid assisted sintering (LAS), may also be affected by the use of MW's.[18] The behavior of the ceramic materials during MWH, and, as a consequence, the resultant effect of the above mentioned phenomena on their sintering, markedly varies, being dependent mostly on the material's electrical and thermal properties. Very large differences exist among ceramic materials regarding these properties.

There are little experimental data regarding MWH of covalent carbides a group of ceramic materials with many practical applications.[19–24] These materials are characterized by high electrical and thermal conductivity, high dielectric loss[25] (in some cases), high melting points and low sinterability. It is not possible to assess the degree of utility of MWH for such materials, based exclusively on theoretical grounds. On one hand, they strongly interact with the MW's, from low temperatures, which allows their direct MW sintering (DMWS) without the use of additional MWH igniters (susceptors). On the other hand, the radiation penetration depth (D_p) is extremely limited. Due to this, only a thin external layer of the specimen is engaged in a strong interaction with the MW's during the last stages of densification, in which the open porosity is low. As a consequence temperature gradients may develop within the specimens with maxima close to the surface.[26]

In this work the feasibility of sintering silicon carbide (SiC), a multifunctional covalent carbide material,[27–31] by MWH was examined. This was done in order to allow one to assess the MWH as an alternative to heating in conventional furnaces (CH). A liquid assisted

* Corresponding author. Tel.: +972-4-8222107/8; fax: +972-4-8325339.
E-mail address: adgold@netuision.net.il (A. Goldstein).

0955-2219/02/$ - see front matter
PII: S0955-2219(01)00498-8

sintering (LAS) approach, with liquids generated by $Al_2O_3 + Y_2O_3$ mixtures,[32–35] was used. This approach gave excellent results when sintering based on conventional heating was used.

2. Experimental procedures

2.1. Processing

Specimens were formed from a powder having a nominal composition of 91 vol.% SiC/1.4 vol.% C/5 vol.% Al_2O_3/2.6 vol.% Y_2O_3. A fine α-SiC powder (grade UF15 of H.C. Starck, Goslar, Germany; specific surface area A≈15 m^2/g, $d_{50} = 0.55$ μm; 1.5% O, 0.03% Al, 0.05% Fe, 0.01% Ca) was the main component of the batch.

Raw material mixing was done by processing for 1 h in an attrition mill (alumina balls, isopropyl alcohol, balls:material ratio ~3). Soft spheroidal pellets were formed after adding PEG 400 (binder/lubricant). The resulting ready-to-press material was obtained by sieving (No. 20 mesh). Green specimens in the shape of discs (diameter $D = 22$–28 mm) or square plates ($l_g = 48$ or 58 mm) were formed by two stage pressing (peak isostatic pressure of 280 MPa). Their bulk green density varied in the $BD_g = 1.8$–1.9 g/cm^3 range. Organic burn-out was done at low temperature, 420 °C/4 h, in order to prevent SiC oxidation. MW sintering was conducted in a furnace operating at 2.45 GHz, using a large multimode applicator ($l = 1.22$ m) with mode stirrer (Model 101 of MMT, Knoxville TN, USA). Specimen temperature was measured with a two-wavelength pyrometer (Mirage of IRCON, Niles, IL, USA) and the atmosphere was Ar/8% N_2. The specimens were placed in a refractory "casket", exhibiting suitable MW transparency, which is shown schematically in Fig. 1. The casket provided the required level of thermal insulation (maximal temperature on its external surface ranged from 600 to 750 °C).

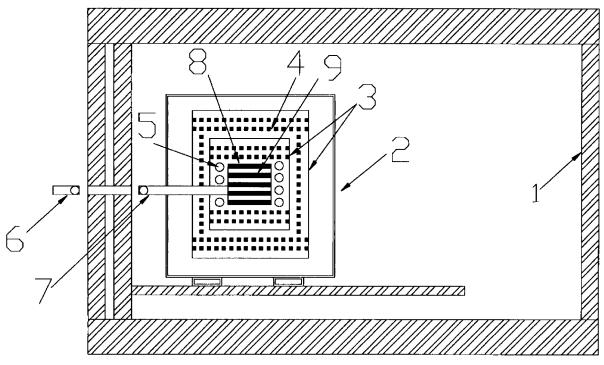

Fig. 1. Schematic representation of the MW heating system. 1—applicator, 2—porous alumina tiles made heating chamber (casket), 3—sintered alumina containers, 4—bubble alumina, 5—SiC grit, 6—pyrometer, 7—alumina tube, 8—sintered alumina specimens container, 9—SiC specimens.

A cylindrical layer of SiC grit (100–500 μm grains; grade Carborex of Orkla Exollon, Norway), having a thickness of ~3 mm, was inserted in the casket in some of the sintering experiments. This layer remains in particulate form even after repeated heatings.

Conventional sintering was conducted in a model 1000A resistive Astro furnace (TT Inc., Santa Rosa, USA).

2.2. Characterization

The bulk density (BD_f) was measured using the Archimedes technique. The overall phase composition was examined by XRD (Philips PW 1720, CuKα). The microstructure, including local elemental and phase composition, was studied by electron microscopy (SEM: Jeol SM 5000; TEM: Jeol 2000 FX; HRTEM: model 3010 UHR Jeol). Grain size was measured applying the lineal intercept method and assuming that the real grain size is $X = 1.56$ L (L = average lineal intercept). Measurements were made from SEM micrographs taken on polished surfaces after etching with Murakami's reagent. The Vickers hardness (H_v) was measured with a DUK IS indenter (Matsuzawa Seiki, Tokyo, Japan). For transversal rupture strength (TRS) measurements, bars (35×4×4 mm) were cut from sintered plates($l_f = 48$ mm) and polished. Measurements were made with a model 1273 testing machine (Instron Corp., Canton MA; four point bending), with a cross-head speed of 0.2 mm/min.[1]

3. Results and discussion

3.1. The MW sintering process. Densification results

Ceramic grades of SiC are extrinsic semiconductors, exhibiting at room temperature considerable electrical conductivity ($\sigma_e = 10$ S m^{-1}) due to the presence of various impurities such as Si, Al, Fe, Mn, etc. The dielectric loss is high with values of $\varepsilon'' > 100$ being measured for the imaginary part of the permittivity.[25] For D_p, values as low as 3 μm have been calculated at 700 °C.[11] A further decrease is expected at sintering temperatures. These data suggest that while SiC is not an ideal material for MWH (low D_p), its MW sintering may be feasible if suitable processing conditions are provided. Below, the results obtained while attempting to densify SiC by MWH are given.

In the case of the MW processing set up used here, pure SiC or $SiC/Al_2O_3 + Y_2O_3$ specimen batches having a mass ⩾25 g could be heated up to ~1950 °C when subjected to the fields produced by forward MW power time profiles in which peak levels of 2.8–4.5 kW were maintained for time periods τ ⩾30 min. An increase of peak power to ~6 kW did not result in further temperature

increases. For a given power profile, no simple correlation between load mass and temperature could be found (maximal loads of ~120 g were tested).

Pure SiC powder compacts heated to 1950 °C (dwell times up to 1 h) did not attain practical levels of densification. The $SiC/Al_2O_3+Y_2O_3$ green specimens, on the other hand, underwent marked densification when subjected to suitable MWH schedules (see Table 1).

It was observed that in order to obtain $BD_f > 90\%$ t.d. (t.d≈3.30 g/cm^3), even for small specimens, temperatures greater than 1880 °C are required. In such conditions advanced densification was obtained both in the presence or absence of the SiC grit. The influence of the SiC grit was felt mostly in the case of the large specimens. The maximal BD_f obtainable could be raised, in the case of the 58 mm green plates, from 93 to 95% t.d. by sintering in the presence of the granular susceptor. The density variations from specimen to specimen, of the same batch, were also reduced together with the tendency to cracking. Yields of 70–80% in uncracked (after sintering) plates could be obtained in a reproducible manner. The insertion of the SiC grit in the casket, modified the approach from pure DMWS to what may be called a hybrid MW heating (HMWH) because heat generated by the grit contributed to the specimen densification. In the set up used here, the porous grit layer has only a moderate shielding effect, so that direct specimen/MW's interaction was possible. This interaction was the main process producing densification.

Fig. 2 presents a MW sintering schedule resulting in advanced densification, after a short dwell time (~30 min) at peak temperatures.

Increase of dwell times (30–90 min range) raised the BD_f of the sintered specimens as indicated in Fig. 3. Further extension of the dwell time to 120–150 min had little effect on BD_f, contributing mostly to grain growth.

The BD_f attained under a given set of sintering conditions was noticeably dependent on the size of the specimens, despite their similar green density. This is also illustrated in Fig. 3. In the case of large plates, shrinkage on the sides of the applicator's median longitudinal plane was non-uniform. This seems to be an indication of MW fields intensity distribution variation on a macroscopic scale. The distribution is MW-system specific; variations are expected as a function of the set-up for a given MW power profile. In the case of the small discs, maximal densification values obtained were $BD_f = 98\%$ t.d. In the case of the intermediate size plates this value decreased to 96% t.d. while for the largest plates the best attainable level of densification, in a reproducible way, was $BD_f = 95\%$ t.d.. Attempts, prior to this work, to sinter by MWH did not succeed in densifying to practical levels (i.e. $BD_f \geqslant 92\%$ t.d.) SiC powder compacts.[19–22] As Table 1 shows, in the case of the large specimens the densification level, attainable by MWH, was lower than that provided by conventional heating. Some MW sintered SiC components are shown in Fig. 4. No effects of size, in the range examined here, on the sintered density of conventionally heated specimens were found.

A mass loss of 4.0–6.5% accompanied the sintering process. The mass loss was not studied here, but it is known that SiC vaporization and its reaction with surface silica—and the liquid producing oxide additives—generate gaseous phases in the temperature range where sintering was done.[32–37]

Table 1
Properties of SiC/Al,Y plates ($l_f = 48$ mm) sintered, 90 min, by the aid of MWH or CH

Characteristics	Heating procedure	
	MWH	CH
Heating conditions (°C/h)	1880–1900/1.5	1900/1.5
BD_f (%t.d.)	95.0	98.5
O.P. (%)	1.2	0.2
H_v (GPa)	22–24	23–25
TRS (MPa)	290–340	370–400

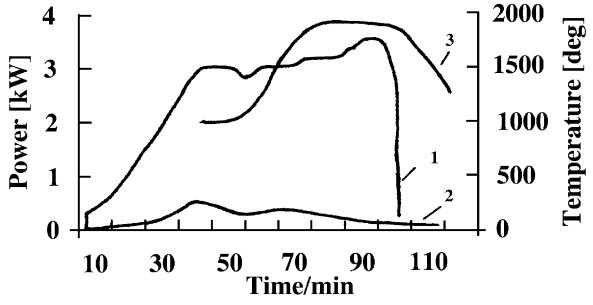

Fig. 2. MW power and temperature time profiles, during a short firing run which resulted in the densification of small specimens (discs having $D = 25$ mm) to $BD_f \approx 92\%$ t.d. 1—forward power, 2—reflected MW power, 3—temperature.

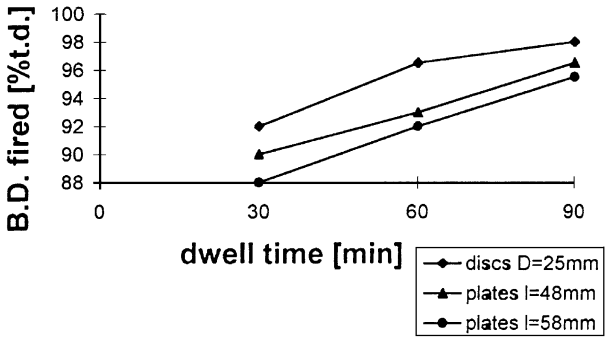

Fig. 3. Dependence of sintered state bulk density on the length of peak temperature dwell time and specimen size.

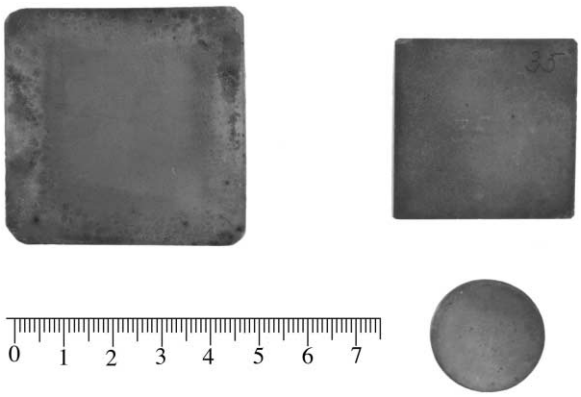

Fig. 4. Various SiC specimens sintered by MW heating.

3.2. Phase composition and microstructure

The XRD patterns showed the presence, in the MW sintered specimens, of α SiC (various polytypes; mostly 6H, 4H and 15R) and the yttrium garnet $3Y_2O_3{\cdot}5Al_2O_3$(YAG). In Fig. 5 a segment from a representative XRD pattern is shown. Amorphous oxide phases, such as those observed by Sigl and Kleebe[34] have not been detected here (TEM examination), neither at SiC grain boundaries nor at carbide/oxide interfaces. In Fig. 6 a typical SiC/YAG interface, as revealed by HRTEM, is shown. The reduction of oxides on the SiC surfaces ($SiO_2 + C$ reaction) eliminates the only oxide glass former present, thus preventing the formation of an amorphous material.[36,37] The excess alumina in the initial composition (relative to YAG stoichiometry) is probably lost by being transformed into gaseous phases by reaction with SiC and/or sublimation.[32,36–38] As a result the yttrium garnet seems to be the only oxide phase present after cooling.

The spatial distribution of the YAG is somewhat different from that observed in specimens conventionally sintered.[34,39] Here, most of the oxide phase is accumulated at triple points or in wide "wedges" present between some of the carbide grains. This morphology is presented in Figs. 7 and 8. Many SiC grain boundaries are free of YAG particles. Such a YAG distribution may be the result of an initial stage of solid state sintering, followed by densification assisted by the liquid phase. High intensity MW fields exist in the region of contact between SiC particles as far as the open porosity remains high.

The carbide appears in the form of fine equiaxed α-SiC grains quite similar to those observed in con-

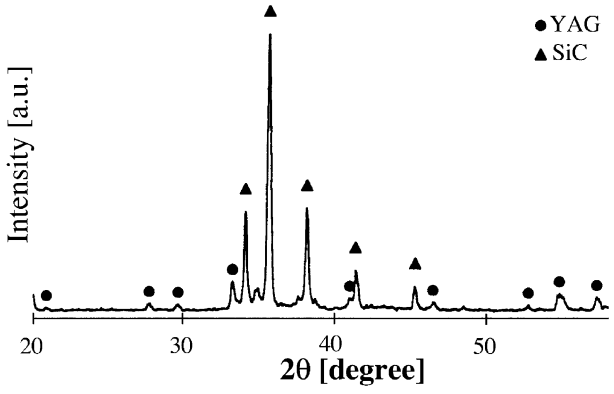

Fig. 5. XRD pattern of sintered SiC/Al–Y–O specimen.

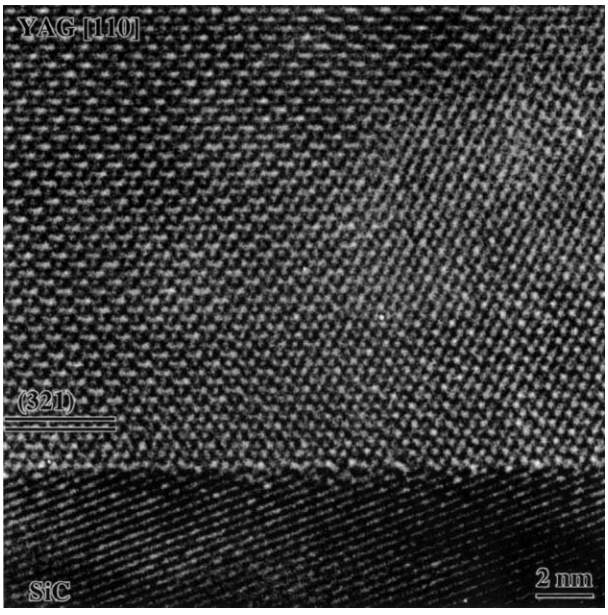

Fig. 6. High resolution TEM micrograph of a SiC–YAG interface.

Fig. 7. Low magnification bright field TEM micrograph of a sintered SiC/Al–Y–O specimen, showing the YAG spatial distribution pattern.

ventionally sintered specimens. The grain size distribution is quite narrow. For instance, a small size disc brought to $BD_f = 97\%$ t.d. (1 h dwell at ~1900 °C) had a mean grain size of $\overline{GS} \sim 0.6$ μm, with all of the grains smaller than 1.5 μm. The specimens sintered in the most energetical conditions (~150 min dwell) still maintained a quite fine grain size ($\overline{GS} \sim 1.2$ μm, $GS_{max} \sim 2.5$ μm).

Fig. 8. Bright field TEM micrograph of a YAG crystal located between α-SiC grains.

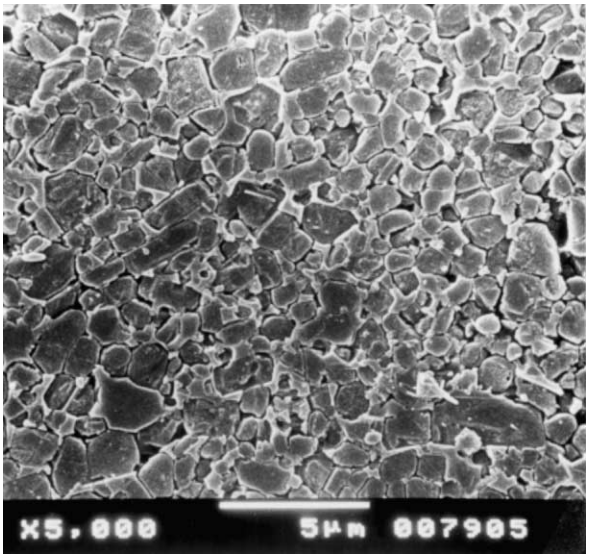

Fig. 9. Low magnification secondary electron SEM micrograph of a sintered SiC/Al–Y–O specimen (150 min dwell at ~1950 °C) showing moderate grain growth.

Fig. 9 shows a low magnification SEM micrograph of the microstructure (specimen brought to $BD_f = 98\%$ t.d. after 150 min dwell).

3.3. Mechanical properties

In Table 1 the values obtained regarding some of the mechanical properties of MW sintered specimens are compared with those of conventionally sintered (1900 °C/1.5 h; Ar) specimens. The average strength of the MW sintered plates is somewhat lower than those of the conventionally fired ones. This is probably due to the lower BD_f of the MWed plates.

4. Summary and conclusions

Despite the low penetration depth of GHz radiation in SiC, at high temperature, it is possible to sinter SiC/$Al_2O_3 + Y_2O_3$ powder compacts by MW heating (2.45 GHz). This is feasible even in the case of "large" specimens ~50 mm in size. The intra-specimen heat generation not withstanding the spatial uniformity of the densification process is not improved in the MWH case. Problems in this sense are created by both the low D_p of SiC and the inherent dynamic macroscopic level variation of the MW field intensity within the applicator's volume. Such features determine, mostly in the case of large specimens, non-uniform shrinkage and/or some reduction of the maximal density obtainable under a given set of heating conditions. Hybrid heating (obtained by insertion of SiC grit in the casket) reduces cracking and improves densification.

BD_f values of up to 98% t.d. (small specimens) could be obtained. For the case of large specimens the level of densification is lower than that obtainable in similar conditions when using conventional heating. The phase composition and to a marked extent also the microstructure and the properties of MW sintered specimens, are similar to those of parts fired in conventional furnaces, in the same temperature range.

While MW sintering (LAS) of SiC provides usable components, it does not seem to generate practical advantages over conventional heating.

References

1. Berteaud, A. J. and Badot, J. C., High temperature microwave heating in refractory materials. *J. Microwave Power*, 1976, **11**, 315–320.
2. Sutton, W.H. and Johnson, W.E., *Method for Microwave Heating*. US Patent No. 4,140,887, 20 February 1979.
3. Janney, M. A. and Kimrey, H. D., Microwave sintering of alumina at 28 GHz. In *Proceedings of the Symp. Ceramic Powder Science II; B, Orlando FL, 1–4 November 1987*, ed. G. L. Messing, E. R. Fuller Jr and H. Hausner. ACerS Pub, Westerville OH, 1988, pp. 919–924.

4. Janney, M. A., Calhoun, C. L. and Kimrey, H. D., Microwave sintering of solid oxide fuel cell materials: I, Zirconia-8 mol% Yttria. *J. Am. Ceram. Soc*., 1992, **75**, 341–346.
5. Sutton, W. H., Microwave processing of ceramic materials. *Am. Ceram. Bull*., 1989, **68**, 376–386.
6. Goldstein, A., Travitzky, N., Singurindi, A. and Kravchik, M., Direct microwave sintering of yttria-stabilized zirconia at 2.45 GHz. *J. Eur. Ceram. Soc*., 1999, **19**, 2067–2072.
7. Goldstein, A., Ruginets, R. and Geffen, Y., Microwave sintering of amorphous silica powders. *J. Mater. Sci. Lett*., 1997, **16**, 310–312.
8. Goldstein, A. and Singurindi, A., Al_2O_3/TiC based metal cutting tools by microwave sintering followed by hot isostatic pressing. *J. Am. Ceram. Soc*., 2000, **83**, 1530–1532.
9. Gerdes, T., Porada, M. W. and Kallasko, R. H., Guidelines of scale-up of MW sintering of hard metals. In *Proc. Symp. Microwaves: Theory and Application in Materials Processing III, Cincinnati OH, 1–3 May 1995*, ed. D. E. Clark, D. C. Folz, S. J. Oda and R. Siberglitt. ACerS Pub, Westerville OH, 1995, pp. 423–431.
10. Binner, J. G. P. and Cross, T. F., Techniques for microstructural control in the microwave sintering of advanced ceramics. *Ceram. Acta*., 1994, **6**, 5–12.
11. Clark, D. E., Microwave processing: present status and future promise. *Ceram. Eng. Sci. Proc*., 1993, **14**, 3–21.
12. Meek, T., Proposed model for the sintering of a dielectric in a microwave field. *J. Mater. Sci. Lett*., 1987, **6**, 638–640.
13. Jhonson Lynn, D. and Rizzo, R. A., Plasma sintering of β''-alumina. *Am. Ceram. Soc. Bull*., 1980, **59**, 467–472.
14. Calame, J. P., Rybakov, K., Carmel, Y. and Ghershon, D., Electric field intensification in spherical neck ceramic microstructure during microwave sintering. In *Proc. Symp. Microwaves: Theory and Application in Materials Processing IV, Orlando FA, 5–9 January 1997*, ed. D. E. Clark, W. H. Sutton and D. A. Lewis. ACerS Pub, Westerville OH, 1997, pp. 135–142.
15. Rybakov, K. I. and Semeonov, V. E., Mass transport in ionic crystals induced by the ponderomative action of a high-frequency electric field. *Physical Review B*, 1995, **52**, 3030–3033.
16. Willert-Porada, M., A microstructural approach to the origin of microwave effects in sintering of ceramics and composites. In *Proc. Symp. Microwaves: Theory and Application in Materials Processing IV, Orlando FA, 5–9 January 1997*, ed. D. E. Clark, W. H. Sutton and D. A. Lewis. ACerS Pub, Westerville OH, 1997, pp. 153–164.
17. Janney, M. A., Kimrey, H. D., Allen, W. R. and Kiggans, J. O., Enhanced diffusion in sappire during microwave heating. *J. Mater. Sci*., 1997, **32**, 1347–1355.
18. Maier, J. and Jamnik, J., Electrochemical processes in ceramics—overview and correlation with microwave effects. In *Proc. Symp. Microwaves: Theory and Application in Materials Processing IV, Orlando FA, 5–9 January 1997*, ed. D. E. Clark, W. H. Sutton and D. A. Lewis. ACerS Pub, Westerville OH, 1997, pp. 123–134.
19. Janney, M. A., Kimrey, H. D. and Kiggans, J. O., Microwave processing of ceramics: guidelines Used at the Oak Ridge National Laboratory. In *Proc. Symp. Microwave Processing of Materials III, San Francisco, CA, 27 April–1 May, 1992*. MRS Publishers, Pittsburgh, PA, 1992, pp. 173–185.
20. Tian, Y. L., Brodwin, M. W., Dewan, H. S. and Johnson Lynn, D., Microwave sintering of ceramics under high gas pressure. In *Proc. Symp. Microwave Processing of Materials, San Francisco, CA*, ed. W. H. Sutton, M. H. Brooks and I. J. Chabinsky. MRS Publishers, Pittsburgh PA, 1988, pp. 213–218.
21. Nesphor, V. S. *et al*., Structure and properties of boron and silicon carbide-base materials obtained by the method of reaction-activated microwave sintering in contact with aluminium nitride. *Prosahkavaya Metallurgya*, 1993, **361**, 83–88.
22. Coughman, J. B. O.etal., Sintering of ceramics using low frequency RF power. In *Proc. Symp. Microwaves: Theory and Application in Materials Processing III, Cincinnati OH, 1–3 May 1995*, ed. D. E. Clark, D. C. Folz, S. J. Oda and R. Siberglitt. ACerS Pub, Westerville OH, 1995, pp. 481–488.
23. Holcombe, C.E. and Morrow, M.S., *Composite of Refractory Material*. US Patent 5,330,942, 19 July 1994.
24. Katz, J. D., Blake, R. D., Petrovic, J. J. and Sheinberg, H., Microwave sintering of boron carbide. In *Proc. Symp. Microwave Processing of Materials, San Francisco, CA*, ed. W. H. Sutton, M. H. Brooks and L. J. Chabinsky. MRS Publishers, Pittsburgh PA, 1988, pp. 219–226.
25. Batt, J. *et al*., A parellel measurement programma in high temperature dielectric property measurements: an update. In *Proc. Symp. Microwaves: Theory and Application in Materials Processing III, Cincinnati OH, 1–3 May 1995*, ed. D. E. Clark, D. C. Folz, S. J. Oda and R. Siberglitt. ACerS Pub, Westerville OH, 1995, pp. 243–250.
26. Koh, M. T. K., Singh, R. K. and Clark, D. E., Temperature distribution considerations during microwave heating of ceramics. In *Proc. Symp. Microwaves: Theory and Application in Materials Processing III, Cincinnati OH, 1–3 May 1995*, ed. D. E. Clark, D. C. Folz, S. J. Oda and R. Siberglitt. ACerS Pub, Westerville OH, 1995, pp. 313–322.
27. Dworak, U., Engineering applications of ceramics. In *High-Tech Ceramics*, ed. G. Kostorz. Academic Press, London, 1989, pp. 115.
28. Aldigner F., Ceramic materials in microelectronics—possibilities and limitations. Ibidem, p. 172.
29. Moulson, A. J. and Herbert, J. M., *Electroceramics*. Chapman and Hall, London, UK, 1990.
30. Kim, Y. and Zangvil, A., Microstructure comparison of transparent and opaque CVD SiC. *J. Am. Ceram. Soc*., 1995, **78**, 1571–1579.
31. Dutta, S., High strength silicon carbides by hot isostatic pressing. In *Proceedings of the 3rd Int. Symp. on Ceramic Mat. and Compo. for Engines, Las Vegas, NV, 27–30 November 1989*, ed. V. J. Tennery. Am Ceram Soc Pub, Westerville OH, USA, 1989, pp. 683–695.
32. Omori, M. and Takei, H., Pressureless sintering of SiC. *J. Am. Ceram. Soc*., 1982, **65**, C–92.
33. Cutler, R. A. and Jackson, T. B., Liquid phase sintered silicon carbide. In *Proceedings of the 3rd Int. Symp. on Ceramic Mat. and Compo. for Engines, Las Vegas, NV, 27–30 November 1988*, ed. V. J. Tennery. Am Ceram Soc Pub, Westerville OH, USA, 1989, pp. 309–318.
34. Sigl, L. and Kleebe, H. J., Core/rim structure of liquid-phase-sintered silicon carbide. *J. Am. Ceram. Soc*., 1993, **76**, 773–776.
35. Liden, E., Carlström, E., Eklund, L., Nyberg, B. and Carlsson, R., Homogeneous distribution of sintering additives in liquid-phase sintered silicon carbide. *J. Am. Ceram. Soc*., 1995, **78**, 1761–1768.
36. Winn, F. J. and Clegg, W. J., Role of the powder bed in densification of silicon carbide sintered with yttria and alumina additives. *J. Am. Ceram. Soc*., 1999, **82**, 3466–3470.
37. Dijen van, F. K. and Mayer, F., Liquid phase sintering of silicon carbide. *J. Eur. Ceram. Soc*., 1996, **16**, 413–420.
38. Mulla, M. A. and Krstic, V., Low temperature pressureless sintering of β-silicon carbide with aluminium oxide and yttrium oxide additions. *Am. Ceram. Bull*., 1991, **70**, 439–443.
39. Böcker, W. and Hamminger, R., Advancements in sintering of covalent high-performance ceramics. *Interceram*, 1991, **40**, 520–524.